

Space Charge Dynamics in a Semiconductor Superlattice Affected by Tilted Magnetic Field and Heating

A. G. Balanov^{1*}, A. A. Koronovskii^{2,3**}, O. I. Moskalenko^{2,3***},
A. O. Selskii^{2,3****}, and A. E. Hramov^{2,3*****}

¹Department of Physics, Loughborough University, Epinal Way, Loughborough LE11 3TU, UK

²Faculty of Nonlinear Processes, Chernyshevskiy Saratov State University,
ul. Astrakhanskaya 83, Saratov, 410012 Russia

³School of Electronic and Mechanical Engineering, Yuri Gagarin State Technical University of Saratov,
ul. Politekhnicheskaya 77, Saratov, 410054 Russia

Received June 17, 2015

Abstract—The transition between different modes of current oscillations in a semiconductor superlattice, from close-to-harmonic (near the generation onset) to relaxation oscillations, has been investigated. The transition type is shown to change with an increase in temperature. A period-doubling bifurcation is observed at low temperatures. With an increase in temperature, the period-doubling bifurcation is observed at increasingly larger values of the voltage across the superlattice. The doubling bifurcation ceases to be observed at voltages at which the generation of oscillations of the current through the semiconductor superlattice is suppressed.

DOI: 10.3103/S1541308X16020035

1. INTRODUCTION

Semiconductor superlattices are structures composed of several thin layers of different semiconductor materials [1–4]. These semiconductor nanostructures are of great interest both for practical applications and for the fundamental science [1, 5–10]. A voltage across a semiconductor sublattice affects the space charge dynamics in it, causing generation of current oscillations due to the formation of electron domains [3, 11]. At the same time, it was shown in [12–15] that a tilted magnetic field affects strongly the electron drift velocities in a superlattice and, as consequence, the space charge dynamics.

At low voltages, the regions with a higher space charge density (electron domains) are stable in time. With an increase in the voltage across the superlattice, the electron domains start moving along the structure. One of the most widespread scenarios leading to generation of current oscillations in a semiconductor superlattice is the normal Andronov–Hopf bifurcation [16]. In this case, the current oscillations are close to harmonic if the critical parameter

(voltage) slightly exceeds the bifurcation value [17]. A further increase in voltage changes significantly the form of current oscillations. In this paper, we report the results of studying the bifurcations caused by the presence of tilted magnetic field and the data on the effect of temperature on the transition between different modes of current oscillations in a semiconductor superlattice. It is shown that the space charge dynamics changes through a period-doubling bifurcation at low temperatures, whereas an increase in temperature leads to suppression of current oscillations in the superlattice.

2. MODEL FOR CALCULATING THE SPACE CHARGE DYNAMICS IN A SEMICONDUCTOR SUPERLATTICE

We will describe the collective space charge dynamics in a semiconductor superlattice using the system of self-consistent continuity and Poisson equations [18]:

$$e \frac{\partial n}{\partial t} = - \frac{\partial J}{\partial x}, \quad (1)$$

$$\frac{\partial F}{\partial x} = \frac{e}{\varepsilon_0 \varepsilon_r} (n - n_D). \quad (2)$$

Here $n(x, t)$ is the electron concentration; $J(x, t)$ is the electric current density; $F(x, t)$ is the current

*E-mail: a.balanov@lboro.ac.uk

**E-mail: alexey.koronovskii@gmail.com

***E-mail: o.i.moskalenko@gmail.com

****E-mail: feanorberserk@gmail.com

*****E-mail: hramovae@gmail.com

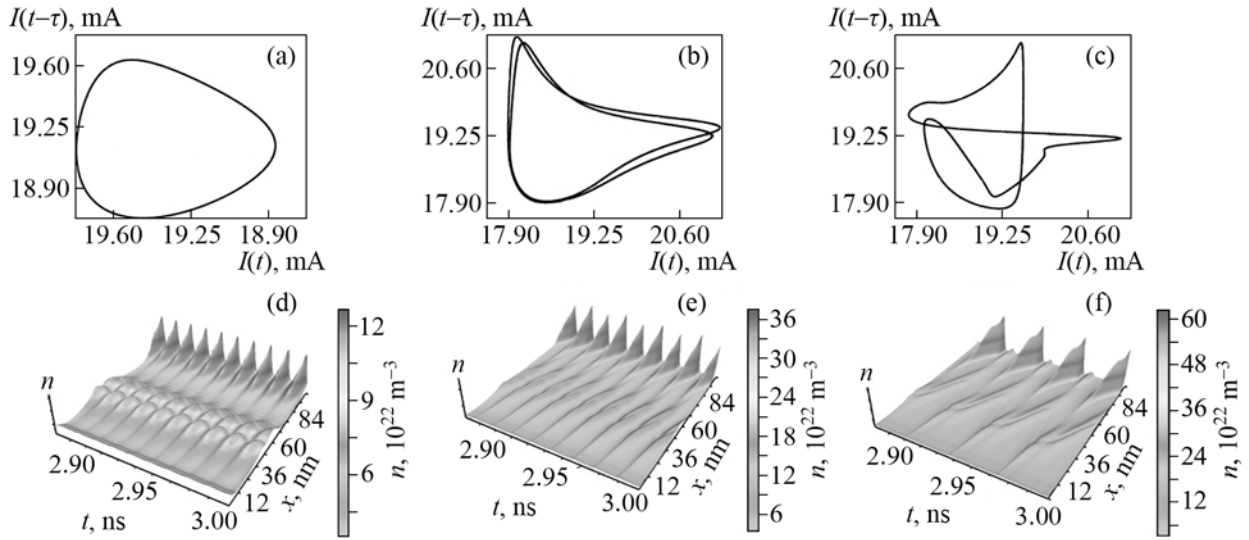


Fig. 1. (a–c) Phase portraits reconstructed by the Takens method (delay time τ is a quarter of the oscillation period) and (d–f) space-time diagrams of the charge carrier concentration; temperature $T = 4.2$ K, tilted magnetic field $B = 15$ T ($\theta = 40^\circ$), and voltage across the semiconductor superlattice $V = 0.565$ (a, d), 0.58 (b, e), and 0.6 V (c, f).

strength; $n_D = 3 \times 10^{22} \text{ m}^{-3}$ is the equilibrium electron concentration; $e > 0$ is the elementary charge; and ϵ_0 and $\epsilon_r = 12.5$ are, respectively, the absolute and relative permittivities.

Within the drift approximation, the current density can be written as

$$J = en v_d(\bar{F}) + eD(\bar{F}) \frac{\partial n}{\partial x}, \quad (3)$$

where $v_d(\bar{F})$ is the electron drift velocity, calculated for mean \bar{F} , and $D(\bar{F})$ is the diffusion coefficient, introduced in correspondence with [3] as

$$D(\bar{F}) = \frac{v_d(\bar{F}) d}{1 - \exp(-e\bar{F}d/kT)} \exp\left(-\frac{e\bar{F}d}{kT}\right). \quad (4)$$

Here, $d = 8.3$ nm is the superlattice period, T is temperature in kelvins, and k is the Boltzmann constant. This diffusion coefficient can be disregarded at low temperatures (few kelvins); at these temperatures and in the absence of tilted magnetic field, the drift velocity is determined by the Esaki–Tsu formula [1]. In the presence of tilted magnetic field, one must use numerical simulation to obtain drift velocities, e.g., in the same way as was described in [15]. The drift velocity decreases with an increase in temperature, whereas the tilted magnetic field gives rise to resonant maxima [14, 15], as a result of which the dynamics of the system becomes much more complicated. In this study, we used a tilted magnetic field with induction $B = 15$ T and tilt angle $\theta = 40^\circ$.

Voltage V applied to a semiconductor superlattice is related to the electric field strength as follows:

$$V = U + \int_0^L F dx, \quad (5)$$

where U is the voltage drop on the contacts (with allowance for the formation of layers with higher charge density near the superlattice emitter and lower charge density near the superlattice collector) and $L = 115.2$ nm is the superlattice length. On the assumption that the emitter and collector contacts are ohmic and the current density J_0 through the emitter is determined by the contact conductivity $\sigma = 3788 \Omega^{-1}$, we have

$$J(0, t) = \sigma F(0, t). \quad (6)$$

3. PERIOD-DOUBLING BIFURCATION

Current oscillations in semiconductor superlattices have relaxation character. However, as was discussed above, at voltages close to the onset of generation caused by the Andronov–Hopf bifurcation, the current oscillations are close to harmonic. To analyze the transition from close-to-harmonic to relaxation oscillations, we will consider the current dynamics and the dynamics of space-time domains (regions with high carrier concentration). The transition between different types of current oscillations can be demonstrated by projecting phase trajectories onto the $(I(t-\tau))$ plane (τ is the delay time, equal to a quarter of the oscillation period), obtained with the aid of Takens method of delays for reconstructing phase portraits based on time realizations [19].

Figure 1 shows projections of phase portraits and spatial and temporal dependences of charge

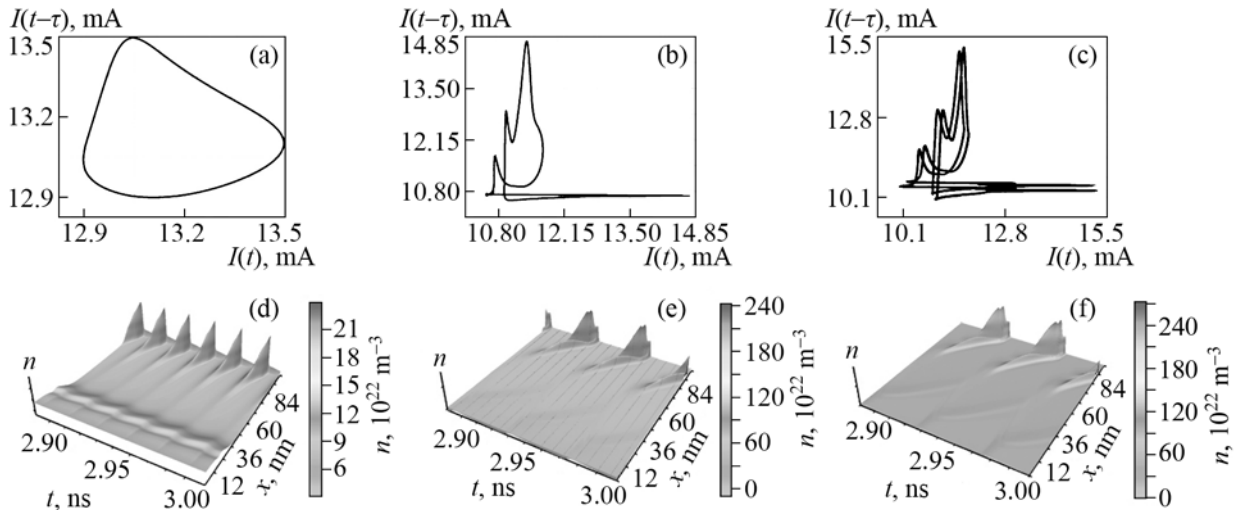


Fig. 2. (a–c) Phase portraits reconstructed by the Takens method (delay time τ is a quarter of the oscillation period) and (d–f) space-time diagrams of the charge carrier concentration; temperature $T = 100$ K, tilted magnetic field $B = 15$ T ($\theta = 40^\circ$), and voltage across the semiconductor superlattice $V = 0.515$ (a, d), 0.615 (b, e), and 0.635 V (c, f).

carrier concentration for different voltages across the semiconductor superlattice at a temperature close to absolute zero ($T = 4.2$ K). For low (close to the generation onset) voltage $V = 0.565$ V, the current oscillations are close to harmonic, and a smooth closed line can be seen in the phase portrait (Fig. 1(a)). Figure 1(d) demonstrates the motion of high-density charge carrier domains, which form ordered patterns. However, an increase in voltage to $V = 0.58$ V changes the dynamics of current and spatial domains. As shown in Figs. 1(b) and 1(e), the limiting cycle is now transformed into a double-period cycle. Hence, a period-doubling bifurcation occurs in the system. Note that this process is accompanied by doubling the oscillation frequency. From the point of view of space-time patterns, this bifurcation manifests itself in domain division along the coordinate when passing the segment from 35 to 80 nm.

One can state that in this case a domain is a combination of two carrier concentration peaks of similar heights because each oscillation period corresponds to one pattern in the space-time diagram. With a further increase in the voltage across the superlattice, the current oscillations even more deviate from harmonic and become even closer to relaxation-type oscillations (Fig. 2(c)). In the space-time diagram of charge carrier concentration, one can see that one of the peaks in the domain decreases, while the other increases (Fig. 2(f)). On the whole, this leads to a decrease in the domain repetition rate (and, as a consequence, to a decrease in the current oscillation frequency, which was discussed above) with an increase in the domain height (the current oscillation amplitude also significantly increases).

Let us consider how an increase in temperature affects the dynamics of current and space-time domains near the period-doubling bifurcation. Figure 2 shows projections of phase trajectories onto the $(I(t-\tau), I(t))$ plane and the space-time diagram of charge carrier concentration at $T = 100$ K. It can be seen that an increase in temperature also gives rise to a period-doubling bifurcation. However, in this case, oscillations are transformed from close-to-harmonic (near the generation onset) (Fig. 2(a)) to close-to-relaxation (Fig. 2(b)), and only after this transformation a period-doubling bifurcation occurs (see Fig. 2(c)). Moreover, the voltage across the superlattice at which the bifurcation is observed is higher than at $T = 4.2$ K. From the point of view of space-time patterns of charge carriers, the transition between oscillation modes at this temperature occurs according to another mechanism. In the previous case ($T = 4.2$ K), two domains merged into one pattern, which changed until one of the initial domains greatly exceeded the other; as a result, the period in the phase portrait for the current was doubled, and a transition between oscillations of different types occurred. With an increase in temperature and voltage, the electron domain is split more rapidly, thus leading to a change in the mode, after which period-doubling bifurcation occurs. These stages are successively shown in Figs. 2(d–f). Before the doubling, the cycle in the phase pattern is not smooth, in contrast to the case of $T = 4.2$ K (compare Figs. 1(b) and 2(c)).

4. SUPPRESSION OF CURRENT OSCILLATIONS

As follows from [15], the amplitude of the resonant peaks in the dependence of the drift velocity

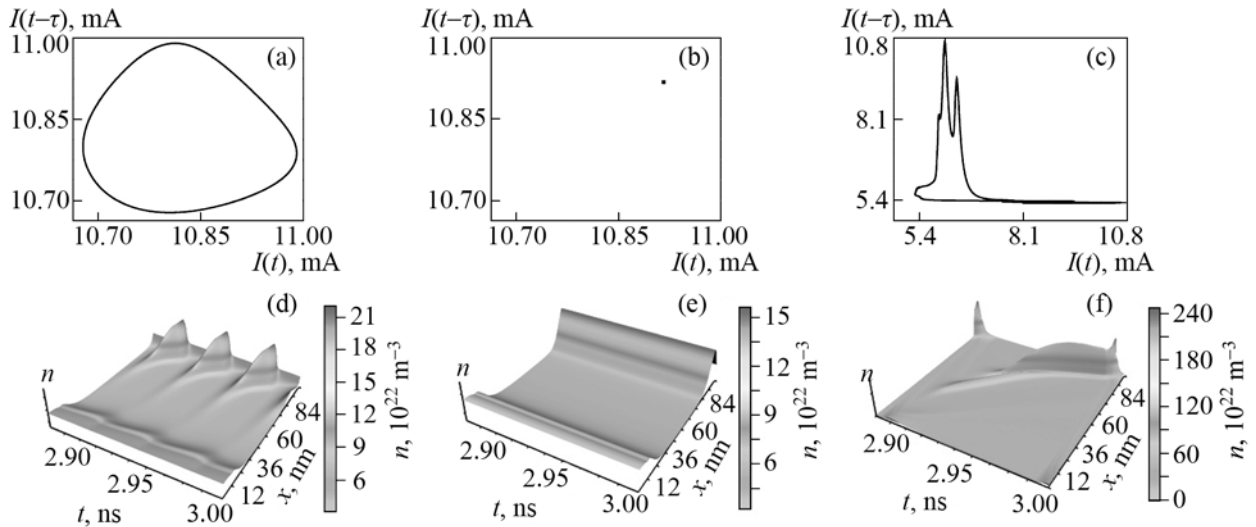


Fig. 3. (a–c) Phase portraits reconstructed by the Takens method (delay time τ is a quarter of the oscillation period) and (d–f) space–time diagrams of the charge carrier concentration; temperature $T = 200$ K, tilted magnetic field $B = 15$ T ($\theta = 40^\circ$), and voltage across the semiconductor superlattice $V = 0.485$ (a, d), 0.565 (b, e), and 0.7 V (c, f).

on the electric field strength may exceed that of the Esaki–Tsu peak as a result of heating. To gain a deeper insight into the nature of the transitions between different modes of current oscillation generation, let us consider the dynamics of the projection of phase trajectories onto the $(I(t-\tau), I(t))$ plane and the behavior of the space–time diagrams of charge carrier concentration with a change in the voltage across the semiconductor superlattice (at $T = 200$ K). It was mentioned above that the generation of oscillations occurs through a Hopf bifurcation, and the oscillations are close to harmonic immediately after the generation onset. This behavior is observed for all temperatures under consideration (see Figs. 1(a), 2(a), 3(a)); the voltage corresponding to the generation onset decreases with an increase in temperature [15]. However, for $T = 200$ K, an increase in voltage to $V = 0.565$ V suppresses the current oscillations in the semiconductor superlattice caused by the inverse Andronov–Hopf bifurcation (Fig. 3(b)). The spatial distribution of charge carriers along the superlattice turns out to be time-independent. An electron domain can be formed along the superlattice; however, it is immobile and does not induce current oscillations (see Fig. 3(b)). Further increase in voltage recovers generation of oscillations (as previously, via a Hopf bifurcation). A period-doubling bifurcation is not observed in this case; however, the oscillation type changes. The type of oscillations depicted in Fig. 3(c) is close to relaxation. The space–time diagram of the charge carrier concentration exhibits the following sequence: a pattern with a single peak, a time-independent pattern, and a complex pattern with several peaks (successively, Figs. 3(d–f)).

5. CONCLUSIONS

We revealed scenarios of transitions between different modes of current oscillations in semiconductor superlattices in the presence of tilted magnetic field, from close-to-harmonic (near the generation onset) to close-to-relaxation ones. The generation of current oscillations due to the motion of electron domains along the structure is implemented both in the presence and in the absence of magnetic field. However, a period-doubling bifurcation (accompanied by a change in the transition between current oscillation modes) may occur in presence of tilted magnetic field. One can conclude that the change in the transition between the oscillation modes is related to the change in the amplitude ratio of the Esaki–Tsu peak and the Bloch cyclotron peaks in the dependence of the drift velocity on the electric field strength, which is observed with an increase in temperature. At low temperatures ($T < 100$ K), a transition occurs through a period-doubling bifurcation, whereas at higher temperatures (e.g., $T = 200$ K) a period-doubling bifurcation is absent; in this case, the transition occurs through suppression of generation associated with the inverse Andronov–Hopf bifurcation.

ACKNOWLEDGMENTS

This study was supported by the Russian Science Foundation, Project 14-12-00222.

REFERENCES

1. L. Esaki and R. Tsu, “Superlattice and Negative Differential Conductivity in Semiconductors,” *IBM J. Res. Develop.* **14**, 61 (1970).

2. A.Y. Shik, "Superlattices-Periodic Semiconductor Structures," *Sov. Phys.-Semicond.* **8**, 1195 (1975).
3. A. Wacker, "Semiconductor Superlattices: A Model System for Nonlinear Transport," *Phys. Rep.* **357**, 1 (2002).
4. R. Tsu, *Superlattices to Nanoelectronics* (Elsevier, Netherlands, 2005).
5. Y. Romanov, "Nonlinear Effects in Periodic Semiconductor Structures," *Optika i Spektroskopiya.* **33**, 917 (1972) [in Russian].
6. A.A. Ignatov and V.I. Shashkin, "Bloch Oscillations of Electrons and Instability of Space-Charge Waves in Superconductor Superlattices," *Sov. Phys.-JETP.* **66**(3), 526 (1987).
7. M. Holthaus, "Collapse of Minibands in Far-Infrared Irradiated Superlattices," *Phys. Rev. Lett.* **69**, 351 (1992).
8. Y. Zhang, J. Kastrup, R. Klann, K.H. Ploog, and H.T. Grahn, "Synchronization and Chaos Induced by Resonant Tunneling in GaAs/AlAs Superlattices," *Phys. Rev. Lett.* **77**, 3001 (1996).
9. T. Hyart, J. Alexeeva, N.V. Mattas, and K.N. Alekseev, "Terahertz Bloch Oscillator with a Modulated Bias," *Phys. Rev. Lett.* **102**, 140405 (2009).
10. A.E. Hramov, A.A. Koronovskii, S.A. Kurkin, V.V. Makarov, M.B. Gaifullin, K.N. Alekseev, N. Alexeeva, M.T. Greenaway, T.M. Fromhold, A. Patané, F.V. Kusmartsev, V.A. Maksimenko, O.I. Moskalenko, and A.G. Balanov, "Subterahertz Chaos Generation by Coupling a Superlattice to a Linear Resonator," *Phys. Rev. Lett.* **112**, 116603 (2014).
11. A.G. Balanov, A.A. Koronovskii, O.I. Moskalenko, A.O. Selskii, and A.E. Hramov, "Effect of Interminiband Tunneling on Complex Processes in a Semiconductor Superlattice," *Phys. Wave Phenom.* **23**(1), 28 (2015) [DOI: 10.3103/S1541308X15010045].
12. T.M. Fromhold, A.A. Krokhin, C.R. Tench, S. Bujkiewicz, P.B. Wilkinson, F.W. Sheard, and L. Eaves, "Effects of Stochastic Webs on Chaotic Electron Transport in Semiconductor Superlattices," *Phys. Rev. Lett.* **87**(4), 046803 (2001).
13. T.M. Fromhold, A. Patané, S. Bujkiewicz, P.B. Wilkinson, D. Fowler, D. Sherwood, S.P. Stapleton, A.A. Krokhin, L. Eaves, M. Henini, N.S. Sankeshwar, and F.W. Sheard, "Chaotic Electron Diffusion Through Stochastic Webs Enhances Current Flow in Superlattices," *Nature.* **428**, 726 (2004).
14. A.G. Balanov, D. Fowler, A. Patané, L. Eaves, and T.M. Fromhold, "Bifurcations and Chaos in Semiconductor Superlattices with a Tilted Magnetic Field," *Phys. Rev. E.* **77**(2), 026209 (2008).
15. A.O. Selskii, A.A. Koronovskii, A.E. Hramov, O.I. Moskalenko, K.N. Alekseev, M.T. Greenaway, F. Wang, T.M. Fromhold, A.V. Shorokhov, N.N. Khvastunov, and A.G. Balanov, "Effect of Temperature on Resonant Electron Transport Through Stochastic Conduction Channels in Superlattices," *Phys. Rev. B.* **84**, 235311 (2011).
16. J. Hizanidis, A.G. Balanov, A. Amann, and E. Schöll, "Noise-Induced Front Motion: Signature of a Global Bifurcation," *Phys. Rev. Lett.* **96**(24), 244104 (2006).
17. A.A. Koronovskii, V.A. Maksimenko, O.I. Moskalenko, A.E. Hramov, K.N. Alekseev, and A.G. Balanov, "Transition to Microwave Generation in Semiconductor Superlattice," *Phys. Wave Phenom.* **21**(1), 48 (2013) [DOI: 10.3103/S1541308X13010093].
18. M.T. Greenaway, A.G. Balanov, E. Schöll, and T.M. Fromhold, "Controlling and Enhancing Terahertz Collective Electron Dynamics in Superlattices by Chaos-Assisted Miniband Transport," *Phys. Rev. B.* **80**, 205318 (2009).
19. F. Takens, *Detecting Strange Attractors in Dynamical Systems and Turbulence, Lectures Notes in Mathematics* (Springler-Verlag, N.Y., 1981).